Original Research *Feature Article*

Altered morpho-functional features of bones in autoimmune disease-prone BXSB/MpJ-*Yaa* mice

Takashi Namba[1], Osamu Ichii[1], Teppei Nakamura[1,2], Md Abdul Masum[1], Yuki Otani[1], Saori Otsuka-Kanazawa[1], Yaser Hosny Ali Elewa[1,3] and Yasuhiro Kon[1]

[1]Laboratory of Anatomy, Department of Basic Veterinary Sciences, Faculty of Veterinary Medicine, Hokkaido University, Sapporo 060-0818, Japan; [2]Section of Biological Safety Research, Chitose Laboratory, Japan Food Research Laboratories, Chitose 066-0052, Japan; [3]Faculty of Veterinary Medicine, Department of Histology and Cytology, Zagazig University, Zagazig 44519, Egypt
Corresponding author: Osamu Ichii. Email: ichi-o@vetmed.hokudai.ac.jp

Impact statement

Bone disease, such as osteoporosis and rheumatoid arthritis, increases because of the progression of an aging society. Autoimmune disease are important and predisposing factors for the pathogenesis of the bone disease; however, the pathological mechanism is unclear. We have demonstrated that systemic autoimmune disease in BXSB/MpJ-*Yaa* is closely associated with the morpho-functional abnormalities of bones including bone marrow and has complicated pathology. The abnormalities are characterized by altered regulations of serum calcium, anemia tendency, and hematopoiesis with increased WBCs and decreased PLs, short length and low mass of long bones, imbalance in the populations of osteoclasts and osteoblasts, and increased expression of candidate genes for causing and/or exacerbating their phenotypes. Therefore, BXSB/MpJ-*Yaa* serves as a model to elucidate bone phenotypes in systemic autoimmune disease that would be affected by the factors in the bone as well as the other immune and/or mineral metabolism organs both in human and experimental medicine.

Abstract

Bones play crucial roles in motility, electrolyte metabolism, and immunity. Clinical cases have suggested bone dysfunction in several systemic autoimmune diseases. This study exhibited altered bone morpho-functions in BXSB/MpJ-*Yaa* as a murine autoimmune disease model. During clinical examinations, the serum Ca level was significantly higher in BXSB/MpJ-*Yaa* than the healthy control BXSB/MpJ at the early stage (two to four months), but that in BXSB/MpJ-*Yaa* decreased with advancing age. Further, the increase of urinary Ca with nephritis and white blood cells with mild anemia proceeded in BXSB/MpJ-*Yaa* with advancing age. The thyroid and parathyroid gland morphologies and serum parathormone level did not differ among strains, but the tibia was smaller in BXSB/MpJ-*Yaa* than in BXSB/MpJ especially during the late stage (six months). Histologically, osteoclasts and osteoblasts showed increased and decreased tendencies, respectively, in BXSB/MpJ-*Yaa* during the early stage, and osteoclasts and bone area significantly increased and decreased, respectively, compared with BXSB/MpJ at later stages. The bone morphological indices were affected by the expression of BXSB/MpJ-*Yaa* mutation genes and inflammatory genes in BXSB/MpJ-*Yaa*. In conclusion, systemic autoimmune diseases in BXSB/MpJ-*Yaa* are associated with the morpho-functional abnormalities of bones, calcium dynamics, and hematopoiesis, and each factor contributes to forming the phenotypes in this disease.

Keywords: Autoimmune disease, BXSB/MpJ-Yaa, bone, calcium, hematology, histopathology

***Experimental Biology and Medicine* 2019; 244: 333–343. DOI: 10.1177/1535370219832810**

Introduction

Bones play various roles, such as assisting motor function and electrolyte metabolism of circulating calcium or phosphorus. Additionally, the bone marrow (BM), a primary lymphatic organ located deep in the bone, plays a crucial role in immunity. To date, the bone and BM have been considered different and unrelated organs owing to the differences in their development and functions. However, recently, the osteoblasts responsible for bone formation were shown to participate in the production of hematopoietic stem and progenitor cells (HSPCs) in mice.[1] Moreover, osteoclast precursor cells and osteoblasts expressed tumor necrosis factor receptor superfamily, member 11a, nuclear

factor kappa B (NFκB) activator (Tnfrsf11a/RANK), and tumor necrosis factor (ligand) superfamily, member 11 (Tnfsf11/RANKL), respectively.[2] This cell to cell contact via RANK/RANKL interaction was important for the differentiation of mouse osteoclast precursor cells into mature osteoclasts.[2] Alternatively, RANKL expression was identified in T-cells. It regulates interactions between T-cells and dendritic cells, maturing dendritic cells, and lymph node organogenesis in humans.[3,4]

The functional imbalance of osteoblasts and osteoclasts causes bone-related diseases such as osteoporosis in humans, and their incidents increase because of the progression of an aging society.[5,6] Osteoporosis and osteopetrosis are associated with the hyper-activation and dysfunction of osteoclasts causing the decrease and increase in bone density, respectively.[6,7] Particularly, aging and altered immune conditions are important and predisposing factors for the pathogenesis of osteoporosis. Rheumatoid arthritis (RA), a bone-related autoimmune disease in humans, causes chronic inflammation characterized by secondary osteoporosis and synovitis, joint swelling, and destruction of cartilage and bone.[8,9] RA patients develop motor impairment with arthralgia, and bone destruction that could be induced by the actions of T helper 1 (Th1)-cells, Th17-cells, B-cells, and produced cytokines, such as tumor necrosis factor α (TNF-α), interleukin 1 (IL-1), and IL-6.[8,10–13] Thus, crucial correlations between the bone and immune system based on osteoimmunology, and their alternations would contribute to their bidirectional pathogenesis.

For the diagnosis and evaluation of bone-related diseases, blood electrolyte examination, targeting Ca and phosphorus, is useful. However, their blood concentration does not completely reflect bone conditions. Blood Ca concentration is regulated by various organs such as bones, thyroid glands, parathyroid glands, kidneys, and intestines with regard to absorption and excretion.[14,15] During the dysfunction of Ca-regulating organs, its blood concentration would be changed. Although the chronic kidney disease (CKD) patients exhibited hypocalcemia and hyperphosphatemia due to impaired renal functions, these imbalances are compensated by an increased activity of parathyroid hormone (PTH). However, with the progression of CKD, PTH cannot control the blood Ca, which shows significant decrease.[16] Further, vitamin D obtained through food, produced in the skin, and activated in the kidney, is related to osteogenesis by increasing blood Ca level.[14] Vitamin D also associates with the immune function and its abnormality. Patients with autoimmune diseases, such as systemic lupus erythematosus (SLE) and RA, have low levels of vitamin D in the blood, contributing to osteoporosis.[17] Furthermore, the blood mineral levels show complex dynamics and do not necessarily represent the state of bones in several diseases. Therefore, the combination of morphological evaluations of bones and blood examinations is essential to understand the pathogenesis of bone-related diseases in the patients suffering the other disease.

To understand the effect of autoimmune diseases on bone morphology, we histopathologically examined the phenotype of BXSB/MpJ-*Yaa* (BXSB-Yaa) mice as an autoimmune disease model. As BXSB-Yaa carries the Y-linked autoimmune accelerator (*Yaa*) mutation on the Y chromosome, the male mice develop severe autoimmune symptoms similar to SLE characterized by abnormal proliferation of B-cells, auto-antibody production, and splenomegaly,[18,19] but not RA.[20] We have already demonstrated the pathological features of nephritis and dacryoadenitis in BXSB-Yaa,[21–23] however, its bone morphology was unclear. Therefore, we analyzed the altered bone structures, especially focusing on the population of osteoblasts and osteoclasts, by comparisons between BXSB-Yaa and its control strain BXSB/MpJ (BXSB) with the evaluation of blood mineral dynamics and autoimmune disease conditions.

Material and methods

Animal ethics

Animal experimentation was approved by the Institutional Animal Care and Use Committee of the Graduate of School of Veterinary Medicine, Hokkaido University (approval no.16–0124). The animals were handled in accordance with the Guide for the Care and Use of Laboratory Animals, Graduate School of Veterinary Medicine, Hokkaido University (approved by the Association for Assessment and Accreditation of Laboratory Animal Care International). Male BXSB and BXSB-Yaa aged two to six months were purchased from Japan SLC, Inc. (Hamamatsu, Japan) and were maintained under specific pathogen-free conditions. Blood of all mice were collected from femoral arteries under deep anesthesia using the mixture of medetomidine (0.3 mg/kg), midazolam (4 mg/kg), and butorphanol (5 mg/kg). Finally, all mice were euthanized by cervical dislocation.

Hematological and serological analysis and urinalysis

The number of white blood cells (WBCs), red blood cells (RBCs), platelets (PLs), hemoglobin concentration (HC), hematocrit volume (Ht), mean corpuscular volume (MCV), and mean corpuscular HC (MCHC) was measured using a XT-1800i instrument (Sysmex Corporation, Kobe, Japan). Additionally, the blood smear was stained by Diff-Quik solution (Sysmex Corporation) to detect reticulocytes.

Serum levels of anti-double strand DNA (dsDNA) antibody were measured to evaluate systemic autoimmune conditions using LBIS Anti dsDNA-Mouse ELISA Kit (FUJIFILM Wako Pure Chemical Corporation, Osaka, Japan) according to the manufacturer's instructions. As an index of mineral metabolism of bones, the serum Ca concentration was measured using a Fuji Dri-Chem 7000v instrument (FUJIFILM Medical Co., Ltd., Tokyo, Japan). Furthermore, urinary concentrations of Ca and creatinine (CRE) were determined by a Fuji Dri-Chem 7000v instrument (FUJIFILM Medical Co., Ltd.) and Creatinine-test-Wako (FUJIFILM Wako Pure Chemical Corporation) according to the manufacturer's instructions. Serum PTH concentration was measured to evaluate parathyroid gland

function using Mouse PTH 1–84 ELISA kit (Quidel Corporation, San Diego, CA, USA).

Morphological and histological analyses of bones

To evaluate the gross morphology of bones, the bone length and wet weight were measured. After taking a picture of the tibia, the tibia length was measured by ImageJ.[24] Subsequently, the ratio of tibia and fibula weight to body weight (BW) was calculated.

The tibia samples for histology were fixed with 4% paraformaldehyde at 4°C overnight, and decalcified by 5% ethylenediaminetetraacetic acid at 4°C for 5 days. After decalcification, the specimens were routinely dehydrated by ethanol and embedded into paraffin. Then, paraffin sections (3 μm) were prepared and stained with hematoxylin and eosin (HE) or tartrate-resistant acid phosphatase (TRAP) staining Kit (FUJIFILM Wako Pure Chemical Corporation) to detect the osteoclasts.

Immunohistochemistry

The paraffin sections were immunostained using the methodology by a previous study.[23] The antigen retrieval was applied to sections (Supplementary Table 1). Subsequently, to block internal peroxidase activity, the sections were soaked in methanol containing 0.3% H_2O_2 for 20 minutes at 25°C. After washing three times in phosphate-buffered saline (PBS), the sections were incubated with a blocking serum for 1 h at 25°C to block the non-specific sites. Then, sections were incubated with primary antibodies overnight at 4°C. The sections were then washed thrice in PBS and incubated with secondary antibodies for 30 minutes at 25°C and washed thrice in PBS. Consequently, the sections were incubated with streptavidin conjugated horseradish peroxidase (SABPO(R) kit, Nichirei; Tokyo, Japan) for 30 minutes at 25°C, washed three times in PBS, and the immunopositive reaction was visualized with 3,3′-diaminobenzidine tetrahydrochloride-H_2O_2 solution. Finally, the sections were lightly stained with hematoxylin. The details of the antibody, antigen retrieval, and blocking are listed in Supplementary Table 1.

Histoplanimetry

We performed the histoplanimetrical analysis of tibias using histological stained sections as shown in Supplementary Figure 1. We evaluated the area ratio of bone to BM, the ratio of trabecular area to tissue area (Tb. Ar/T.Ar), trabecular width (Tb.Wi), trabecular number (Tb. N), trabecular separation (Tb.Sp), $TRAP^+$ cells with 2 or more nuclei, as osteoclasts, $osteocalcin^+$ cells, osteoblasts, and osteocytes.[25,26]

Quantitative polymerase chain reaction

Total RNA from the bone including BM in a humerus was purified using the TRIzol reagent (Thermo Fisher Scientific, Waltham, MA, USA) following the manufacturer's instructions. The purified total RNA (83.3 ng/μl) was treated as a template to synthesize cDNA using ReverTra Ace qPCR RT Master Mix (Toyobo Co., Ltd., Osaka, Japan). Quantitative polymerase chain reaction (qPCR) analysis was performed on the cDNA (20 ng/μl) using THUNDERBIRD® SYBR® qPCR Mix (Toyobo Co., Ltd.) and the following gene-specific primers (Supplementary Table 2). The qPCR cycling conditions were: 95°C for 1 min, (95°C for 15 s, 60°C for 45 s (40 cycles)). Data were normalized by the values of actin, beta (*Actb*), and those of BXSB at three months using the delta-delta Ct method.

Statistical analysis

The data were expressed as the mean ± standard error (SE) and statistically analyzed by a non-parametric manner. Briefly, the significance between the two groups was analyzed by the Mann–Whitney *U*-test ($P < 0.05$). The correlation between the two parameters was analyzed using Spearman's correlation test ($P < 0.05$).

Results

Autoimmune disease features found in BXSB-Yaa

We pathologically examined mice at three and six months of age (Figure 1). The BW in BXSB-Yaa was lower than in BXSB at both ages, and that of BXSB significantly increased with advancing age, but not in BXSB-Yaa (Figure 1(a)). Regarding autoimmune disease indices, BXSB-Yaa showed significantly higher values in the ratio of spleen weight to BW (S/B) and the serum levels of anti-dsDNA antibody compared with BXSB at both ages (Figure 1(b) and (c)). Further, for S/B, BXSB-Yaa at six months significantly showed higher values than those at three months (Figure 1(b)). Thus, autoimmune disease phenotypes were evident in BXSB-Yaa and deteriorated at six months.

Impaired bone metabolism, renal function, and hematopoiesis in BXSB-Yaa

Considering bone metabolism indices, the serum level of Ca was significantly higher in BXSB-Yaa than in BXSB at two to four months, and that of the former was significantly decreased with advancing age (Figure 1(d)), indicating the imbalanced Ca metabolism in BXSB-Yaa. For the ratio of urinary Ca to CRE level, an indicator of urinary Ca excretion, the BXSB-Yaa at six months showed the highest value, and significant differences were observed between three and six months in this strain (Figure 1(e)). Although we hypothesized secondary hyperparathyroidism in BXSB-Yaa at six months due to nephritis,[14] neither significant age- nor strain-related change was observed in the serum PTH concentration (Figure 1(f)).

Furthermore, we performed hematological and serological analyses, focusing on hematopoiesis including, counts of WBCs, RBCs, PLs (Figure 1(g) to (i)), HC, Ht, MCV, and MCHC (Figure 1(j) to (m)). BXSB-Yaa showed significant increase and decrease in WBCs and PLs at six months compared with three months, respectively (Figure 1(g) and (i)). Further, BXSB-Yaa at six months showed significant increase and decrease in MCV and MCHC compared with BXSB at the same age, respectively (Figure 1(l) and (m)). There was no significant age- or strain-related change in the

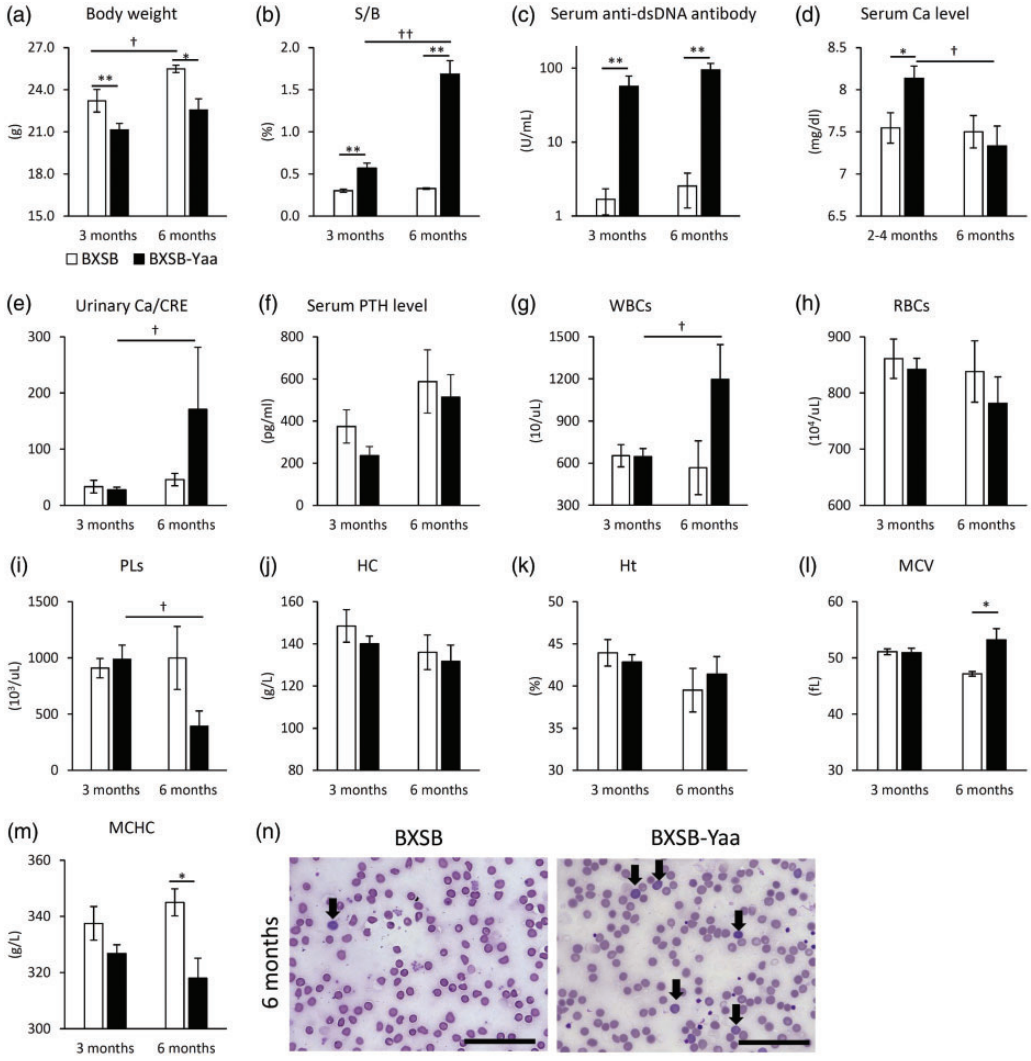

Figure 1. Autoimmune disease-associated phenotypes, serological and hematological analysis, and urinalysis in mice. (a) Body weight (BW). (b) The ratio of spleen weight to BW (S/B). (c) The serum levels of anti-double strand DNA (dsDNA) antibody. (d) Serum calcium (Ca) level. (e) The ratio of urinary Ca to creatinine (CRE) level. (f) Serum parathyroid hormone (PTH) level. (g) The number of white blood cells (WBCs). (h) The number of red blood cells (RBCs). (i) The number of platelets (PLs). (j) Hematocrit concentration (HC). (k) Hematocrit volume (Ht). (l) Mean corpuscular volume (MCV). (m) Mean corpuscular HC (MCHC). (n) Blood smear. Some reticulocytes (arrows) are observed in the smear of BXSB-Yaa at six months. Diff-Quik staining. Bars = 50 μm. BXSB: BXSB/MpJ. BXSB-Yaa: BXSB/MpJ-*Yaa*. The numbers of samples used in the studies are as follows: n = 8–18 (a and b), n = 5–10 (c), n = 9–16 (d), n = 5 (e), n = 8–18 (f), and n = 4–9 (g to m). Each bar represents the mean ± SE. *Significance with the other strain at the same age (Mann–Whitney *U*-test, $^{*}P < 0.05$, $^{**}P < 0.01$). †Significance with the same strain at other age (Mann–Whitney *U*-test, $^{\dagger}P < 0.05$, $^{\dagger\dagger}P < 0.01$). (A color version of this figure is available in the online journal.)

other parameters. Further, at six months, the reticulocytes were more abundant in BXSB-Yaa than in BXSB (Figure 1(n)).

We also histologically examined the organs, such as kidneys, thyroid and parathyroid glands, involved in the regulation of blood Ca concentration (Figure 2(a) to (c)). For renal histopathology, severe glomerulonephritis with immune cell infiltrations to the tubulointerstitium was observed in the kidney of BXSB-Yaa at six months as described previously,[21] but that was not clearly observed in BXSB at both ages and BXSB-Yaa at three months (Figure 2(a)). The injured kidney in BXSB-Yaa at six months coincided with increase in urinary Ca level (as shown in Figure 1(e)). In thyroid glands, histopathological changes such as dilation of follicle or inflammation were not observed in all examined mice (Figure 2(b)). Further, the localization and the number of immune-positive parafollicular cells for calcitonin, which decreases blood Ca level by inhibiting bone resorption, did not remarkably differ. Parathyroid glands were similarly observed among all examined mice, and were surrounded by the connective tissues in thyroid glands (Figure 2(c)). Similar to thyroid glands, no histopathological change including inflammation was observed within the parathyroid glands in all mice. Further, the localization and the number of immune-positive principal cells for PTH, increasing bone resorption, did also not remarkably differ.

Altered bone morphology in BXSB-Yaa

Macroscopically, during observation periods, the tibia of BXSB-Yaa were smaller, and BM was whiter compared to BXSB at six months (Figure 3(a)) as associating with the

increased WBCs and anemic phenotypes of BXSB-Yaa (Figure 1(g), (l) and (n)). The tibia length and the weight of tibia and fibula significantly increased in BXSB with advancing age, but an age-related significant increase in BXSB-Yaa was only observed in the tibia length (Figure 3 (b) and (c)). Importantly, BXSB-Yaa exhibited significantly shorter and lighter tibia compared to BXSB at six months (Figure 3(b) and (c)). Further, the ratio of tibia and fibula weight to BW in BXSB-Yaa at six months was significantly lower than in the same strain at three months or BXSB at six months (Figure 3(d)).

Regarding the histopathological analysis of the tibias, we observed entire bone sections and identified drastic morphological changes around the epiphysis in BXSB-Yaa. Briefly, although no remarkable strain difference was observed at three months, the reduction of trabeculas and thinning of compact bone was observed in BXSB-Yaa at six months (Figure 3(e)). In the area ratio of bone to BM, an indicator of bone thickness, BXSB-Yaa showed significantly lower values compared with BXSB at six months (Figure 3 (f)). Further, to evaluate trabecular bones, we examined Tb. Ar/T.Ar, Tb.Wi, Tb.N, and Tb.Sp, according to a parallel plate model (Figure 3(g) to (j)).[25,26] Regarding the values of Tb.Ar/T.Ar, Tb.Wi, and Tb.N, BXSB-Yaa at six months of age showed significantly lower values compared with the same strain at three months or BXSB at six months of age, and Tb.Wi in BXSB-Yaa at three months was also significantly lower than BXSB at the same age (Figure 3 (g) to (j)). Additionally, BXSB-Yaa at six months of age showed significantly higher values in Tb.Sp compared with BXSB-Yaa at three months and BXSB at six months of age (Figure 3 (j)). However, no significant difference was observed in the density of osteocytes between the strains at both examined ages (Figure 3(k)).

Altered number of osteogenesis-associated cells in BXSB-Yaa

To evaluate osteoclasts, we observed the cells positive for TRAP, the enzyme produced by osteoclasts.[27] $TRAP^+$ osteoclasts were mainly localized to the surface of the medullary cavity, and were more abundant near the epiphyseal cartilages in both strains at both ages (Figure 4(a)). However, the enzyme activity of TRAP seemed to be stronger in BXSB-Yaa at six months compared with other mice. These findings were confirmed by histoplanimetry, displaying that the number of $TRAP^+$ osteoclasts was higher in BXSB-Yaa than in BXSB at both ages, and significant difference was observed at six months (Figure 4(c)).

Subsequently, we also evaluated osteoblasts by immunohistochemistry targeting the osteocalcin produced by osteoblasts, which is generally regarded as a marker of bone formation.[28] Similar to $TRAP^+$ osteoclasts, the $osteocalcin^+$ cells lined the surface of the medullary cavity (Figure 4(b)). There were no age- or strain-related differences in the numerical values of osteoblasts. However, BXSB-Yaa tended to display lower values compared to BXSB at three months of age, and subsequently tended to increase with advancing age, in the $osteocalcin^+$ osteoblasts (Figure 4(d)).

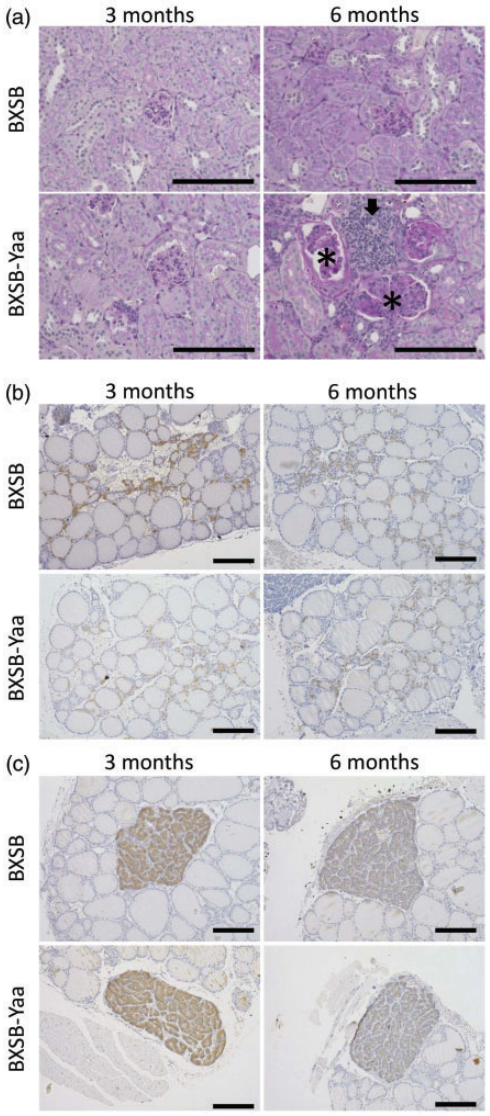

Figure 2. Histology of thyroid and parathyroid glands in mice. (a) Renal histology. Severe glomerulonephritis (asterisks) and cell infiltrations into the tubulointerstitium (arrow) are observed in the kidneys of BXSB-Yaa at six months. PAS staining. (b) Thyroid glands. Immunohistochemistry for calcitonin. Neither age- nor strain-related changes are observed in the organ. (c) Parathyroid glands. Immunohistochemistry for parathyroid hormone. Neither age- nor strain-related changes are observed in each organ. BXSB: BXSB/MpJ. BXSB-Yaa: BXSB/MpJ-*Yaa*. The number of samples used in the studies is as follows: n = 4 (a), n = 5–12 (b), and n = 4–8 (c). Bars = 100 μm. (A color version of this figure is available in the online journal.)

mRNA expression of Yaa locus genes and inflammatory cytokines in BXSB-Yaa

In order to identify the factors associated with autoimmune disease and bone abnormalities, the mRNA expression of the humerus including BM was examined by qPCR. Firstly, we examined the genes on the *Yaa* locus (Figure 5), since BXSB-Yaa had the duplicated 15 genes on Y chromosome because of translocation of X chromosome.[19] The genes, such as Rab9, member of the RAS oncogene family (*Rab9*), tymosin β 4 X chromosome (*Tmsb4x*), phosphoribosyl pyrophosphate synthetase 2 (*Prps2*), toll-like receptor 7 (*Tlr7*), and *Tlr8*, were higher in BXSB-Yaa compared with BXSB at three and six months of ages without age-related

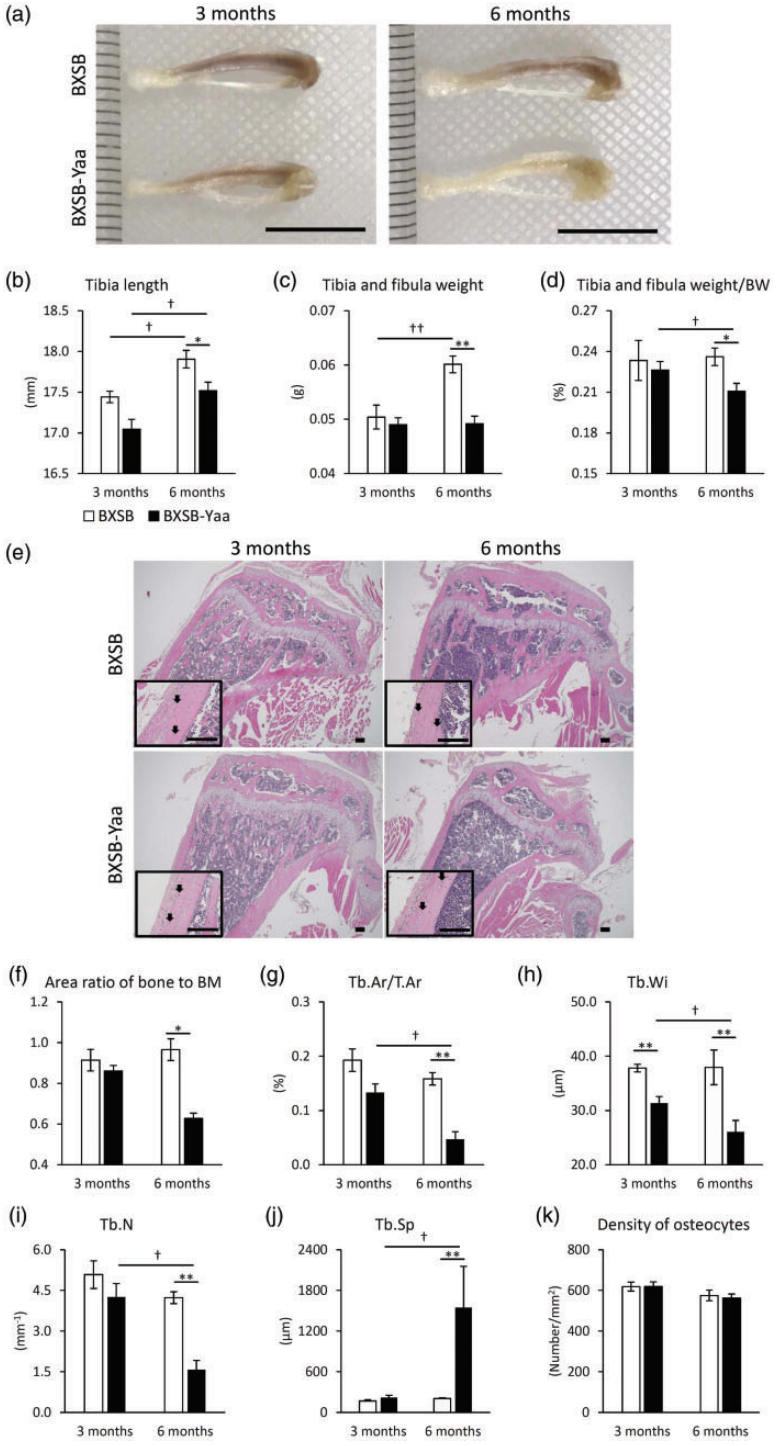

Figure 3. Morphological differences of bones in mice. (a) Gross morphology of bones. At six months, the tibia and fibula of BXSB/MpJ-*Yaa* (BXSB-*Yaa*) is macroscopically smaller, and its bone marrow (BM) is whiter compared with BXSB/MpJ (BXSB). Bars = 10 mm. (b) Tibia length. (c) Tibia and fibula weight. (d) The ratio of tibia and fibula weight to body weight (BW). (e) Tibia histology. The reduction of trabeculas and thinning of compact bone are observed in BXSB-Yaa at six months. Neither age- nor strain-related differences in the number of osteocytes (arrows) are observed. HE staining. Bars = 100 μm. (f) The area ratio of bone to bone marrow (BM). (g) The ratio of trabecular area to tissue area (Tb.Ar/T.Ar). (h) Trabecular width (Tb.Wi). (i) Trabecular number (Tb.N). (j) Trabecular separation (Tb.Sp). (k) The density of osteocytes. BXSB: BXSB/MpJ. BXSB-Yaa: BXSB/MpJ-*Yaa*. The number of samples used in the studies is as follows: n = 4–14. Each bar represents the mean ± SE. *Significance with the other strain at same age (Mann–Whitney *U*-test, $^{*}P < 0.05$, $^{**}P < 0.01$). †Significance with the same strain at other age (Mann–Whitney *U*-test, $^{\dagger}P < 0.05$, $^{\dagger\dagger}P < 0.01$). (A color version of this figure is available in the online journal.)

changes. Thus, the expression of the genes seemed to be increased by the influence of *Yaa* mutation. Further, BXSB-Yaa significantly showed higher expression in MSL complex subunit 3 (*Msl3*) and Rho GTPase activating protein 6 (*Arhgap6*) compared with BXSB at six months and BXSB-Yaa at three months. An age-related significant increase was observed in the expression of amelogenin X-linked (*Amelx*) in BXSB-Yaa, and this strain at six

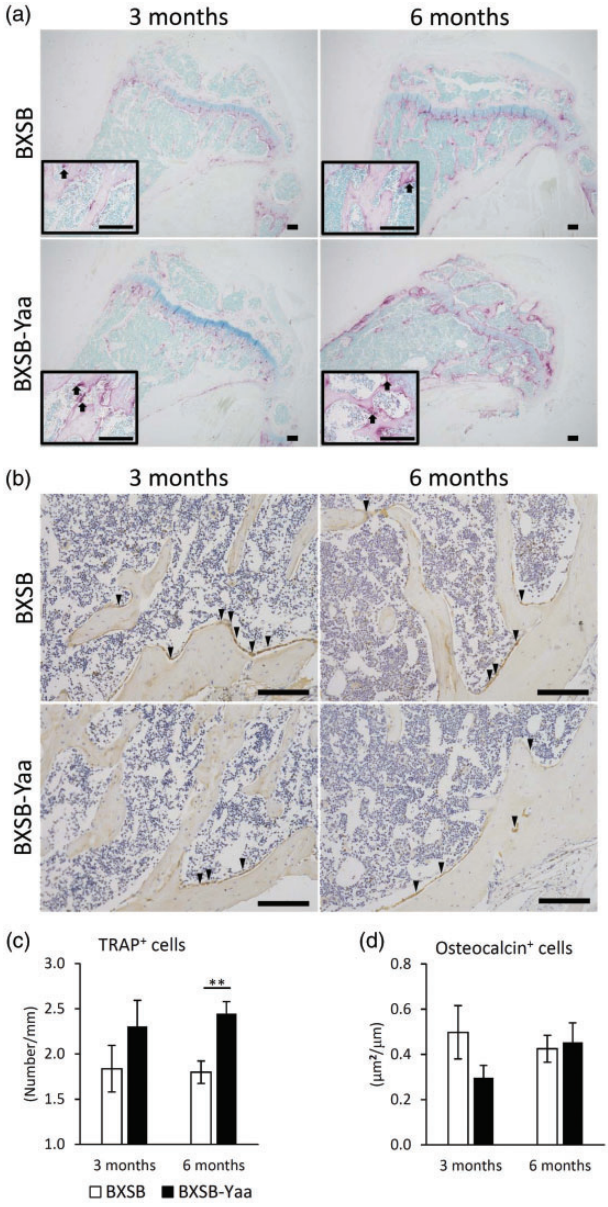

Figure 4. Altered number of osteoclasts and osteoblasts in mouse bones. (a) Tibia histology stained by tartrate-resistant acid phosphatase (TRAP) for osteoclast detection. TRAP$^+$ osteoclasts (arrows) in all mice are mainly localized to the surface of the medullary cavity, especially near the epiphyseal cartilages, and seem to elicit a stronger reaction in BXSB-Yaa at six months compared with the other mice. (b) Tibia histology stained by immunohistochemistry of osteocalcin for osteoblasts. The numerical values of osteocalcin$^+$ osteoblasts (arrow heads), also localized to surface of medullary, seems to be lesser in BXSB-Yaa compared with BXSB at three months. (c) The number of positive cells for TRAP. (d) The numerical values of positive cells for osteocalcin. BXSB: BXSB/MpJ. BXSB-Yaa: BXSB/MpJ-*Yaa*. Bars = 100 μm. The number of samples used in the studies is as follows: n = 5–12. Each bar represents the mean ± SE. *Significance with the other strain at the same age (Mann–Whitney *U*-test, $P < 0.05$). (A color version of this figure is available in the online journal.)

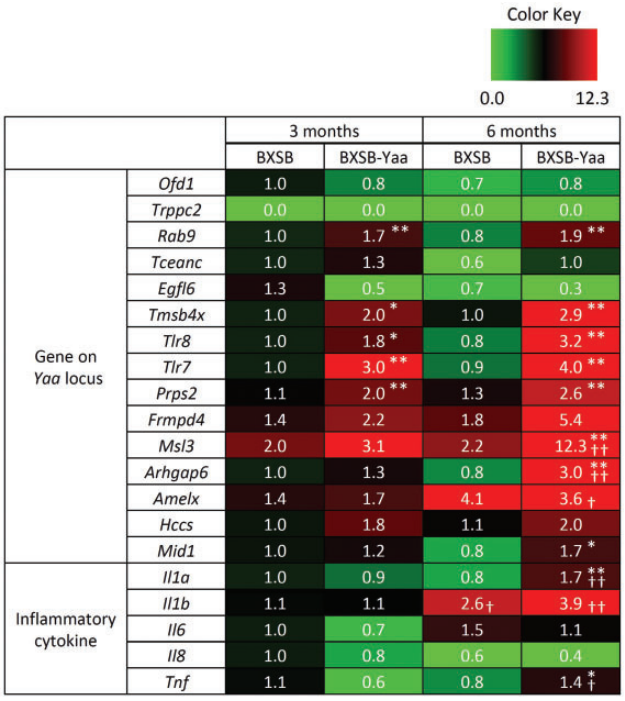

		3 months		6 months	
		BXSB	BXSB-Yaa	BXSB	BXSB-Yaa
Gene on *Yaa* locus	*Ofd1*	1.0	0.8	0.7	0.8
	Trppc2	0.0	0.0	0.0	0.0
	Rab9	1.0	1.7 **	0.8	1.9 **
	Tceanc	1.0	1.3	0.6	1.0
	Egfl6	1.3	0.5	0.7	0.3
	Tmsb4x	1.0	2.0 *	1.0	2.9 **
	Tlr8	1.0	1.8 *	0.8	3.2 **
	Tlr7	1.0	3.0 **	0.9	4.0 **
	Prps2	1.1	2.0 **	1.3	2.6 **
	Frmpd4	1.4	2.2	1.8	5.4
	Msl3	2.0	3.1	2.2	12.3 ** ††
	Arhgap6	1.0	1.3	0.8	3.0 ** ††
	Amelx	1.4	1.7	4.1	3.6 †
	Hccs	1.0	1.8	1.1	2.0
	Mid1	1.0	1.2	0.8	1.7 *
Inflammatory cytokine	*Il1a*	1.0	0.9	0.8	1.7 ** ††
	Il1b	1.1	1.1	2.6 †	3.9 ††
	Il6	1.0	0.7	1.5	1.1
	Il8	1.0	0.8	0.6	0.4
	Tnf	1.1	0.6	0.8	1.4 * †

Figure 5. mRNA expression of *Yaa* locus genes and inflammatory cytokines in the bones of mice. The genes on *Yaa* locus, such as *Rab9*, *Tmsb4x*, *Tlr8*, *Tlr7*, and *Prps2*, are higher in BXSB-Yaa compared with BXSB at both ages. Additionally, BXSB-Yaa at six months also significantly shows higher expression in *Msl3* and *Arhgap6* compared with BXSB and BXSB-Yaa at three months, respectively. Age-related significant increase is observed in the expression of *Amelx* in BXSB-Yaa, and this strain at six months also significantly shows higher expression in *Mid1* than BXSB. The mRNA levels of inflammatory cytokines, such as *Il1a* and *Tnf*, in BXSB-Yaa at six months are significantly higher than in BXSB at the same age and in BXSB-Yaa at three months. Further, an age-related significant increase is observed in the mRNA levels of *Il1b* in both strains. BXSB: BXSB/MpJ. BXSB-Yaa: BXSB/MpJ-*Yaa*. The number of samples used in the studies is as follows: n = 5–15. Each bar represents the mean ± SE. *Significance with the other strain at the same age (Mann–Whitney *U*-test, $*P < 0.05$, $**P < 0.01$). †Significance with the same strain at other ages (Mann–Whitney *U*-test, $^{\dagger}P < 0.05$, $^{\dagger\dagger}P < 0.01$). (A color version of this figure is available in the online journal.)

months also significantly showed higher expression in Midline 1 (*Mid1*) than BXSB at the same age.

Consequently, the mRNA levels of inflammatory cytokines associating with bone resorption, such as *Il1a*, *Il1b*, *Il6*, *Il8*, and *Tnf*, were measured (Figure 5).[10–12,29] The expression of *Il1a* and *Tnf* in BXSB-Yaa at six months was significantly higher than in BXSB at six months and in BXSB-Yaa at three months. Furthermore, the mRNA levels of *Il1b* in both strains at six months were higher than that at three months, and the increase of BXSB-Yaa was more significant.

Correlation between altered bone morphology and autoimmune disease in BXSB-Yaa

Correlation between the indices of bone morphology and autoimmune disease is shown in Table 1. The ratio of tibia and fibula weight to BW in all mice showed significant and negative correlations with S/B and mRNA expression of *Tlr8* and *Tlr7* in bones; and that in BXSB-Yaa showed significant and negative correlations with *Arhgap6* expression in bones. The area ratio of bone to BM showed significant and negative correlations with serum anti-dsDNA antibody levels and mRNA expression of *Rab9*, *Tmsb4x*, *Prps2*, *Msl3*, *Arphgap6*, and *Mid1* in bones; and that in BXSB-Yaa showed significant and negative correlations with *Tmsb4x*, *Prps2*, and *Msl3* expression in bones. Tb.Ar/T.Ar showed significant and negative correlations with S/B, serum anti-dsDNA antibody levels, and mRNA expression of *Tmsb4x*, *Tlr7*, *Tlr8*, *Prps2*, *Msl3*, *Arphgap6*,

Table 1. Correlations between bone morphological parameters and autoimmune disease indices or gene expression.

		Parameters					
	Strains	TF/B	Bone area	Tb.Ar/T.Ar	Tb.Wi	Osteoclast	Osteoblast
S/B	All mice	−0.407*	0.117	−0.660**	−0.665**	0.470**	−0.01
	BXSB-Yaa	−0.144	0.401	−0.476*	−0.399	0.161	0.074
Anti-dsDNA antibody	All mice	−0.331	−0.523*	−0.621**	−0.452*	0.702**	0.079
	BXSB-Yaa	−0.233	0.048	0.033	0.300	0.583	0.314
Ofd1	All mice	0.321	−0.296	−0.049	0.092	−0.218	−0.01
	BXSB-Yaa	0.771	−0.214	−0.095	−0.738*	−0.619	−0.214
Rab9	All mice	−0.100	−0.591**	−0.259	−0.680**	0.094	0.022
	BXSB-Yaa	0.600	−0.310	−0.095	−0.762*	−0.738*	−0.071
Tceanc	All mice	−0.132	−0.286	−0.236	−0.534*	0.230	−0.179
	BXSB-Yaa	0.029	0.071	−0.286	−0.238	0.238	−0.036
Egfl6	All mice	−0.312	0.263	0.032	0.238	0.082	0.091
	BXSB-Yaa	−0.257	0.476	0.048	0.500	0.381	−0.357
Tmsb4x	All mice	−0.056	−0.575*	−0.397*	−0.684**	0.288	−0.221
	BXSB-Yaa	0.371	−0.738*	−0.524	−0.881**	−0.619	0.250
Tlr8	All mice	−0.449*	−0.050	−0.574**	−0.618**	0.539**	0.054
	BXSB-Yaa	−0.181	0.091	−0.389	−0.221	0.276	0.005
Tlr7	All mice	−0.399*	0.175	−0.397*	−0.684**	0.288	−0.221
	BXSB-Yaa	0.011	0.456	−0.221	−0.482	0.009	−0.670*
Prps2	All mice	−0.282	−0.558*	−0.585*	−0.686**	0.399	0.216
	BXSB-Yaa	0.429	−0.738*	−0.5	−0.524	−0.095	0.286
Frmpd4	All mice	−0.240	−0.432	−0.318	0.071	0.393	0.231
	BXSB-Yaa	−0.486	−0.607	−0.214	0.000	0.143	0.486
Msl3	All mice	−0.188	−0.639**	−0.544*	−0.364	0.488*	0.223
	BXSB-Yaa	−0.600	−0.929**	−0.667	−0.429	0.024	0.357
Arhgap6	All mice	−0.418	−0.577*	−0.505*	−0.377	0.680**	0.093
	BXSB-Yaa	−0.886*	−0.595	−0.357	0.143	0.619	0.750
Amelx	All mice	−0.086	−0.047	−0.038	0.350	0.224	0.600*
	BXSB-Yaa	−0.657	−0.69	−0.476	0.048	0.452	0.571
Hccs	All mice	0.018	−0.444	−0.36	−0.495*	0.159	0.132
	BXSB-Yaa	0.200	−0.357	−0.143	−0.548	−0.381	−0.071
Mid1	All mice	−0.276	−0.585*	−0.255	−0.327	0.486*	0.152
	BXSB-Yaa	−0.657	−0.333	−0.167	0.071	0.500	0.714
Il1a	All mice	−0.252	0.212	−0.326	−0.444*	0.010	0.154
	BXSB-Yaa	−0.133	0.362	−0.550*	−0.536*	−0.124	0.143
Il1b	All mice	−0.306	0.225	−0.579**	−0.440*	0.111	0.072
	BXSB-Yaa	−0.125	0.159	−0.554*	−0.468	−0.041	0.214
Il6	All mice	0.385	0.265	0.051	0.036	−0.294	0.100
	BXSB-Yaa	−0.200	−0.429	−0.619	−0.714*	−0.214	−0.100
Il8	All mice	0.046	−0.017	0.235	0.078	−0.142	−0.236
	BXSB-Yaa	0.700	0.25	0.143	−0.643	−0.357	−0.600
Tnf	All mice	−0.050	−0.066	0.026	0.037	0.047	0.056
	BXSB-Yaa	−0.432	−0.095	−0.218	−0.024	0.037	0.136

BXSB-Yaa: BXSB/MpJ-Yaa, S/B: Ratio of spleen weight to body weight, TF/B: Ratio of tibia and fibula weight to body weight, Bone area: Area ratio of bone to bone marrow, Tb.Ar/T.Ar: The ratio of bone area to tissue area, Tb.Wi: Trabecular width, Tb.N: Trabecular number, Tb.Sp: Trabecular separation, Osteoclasts: Number of TRAP+ osteoclasts, Osteoblasts: Numerical values of osteocalcin+ osteoblasts.
Spearman's rank correlation coefficients: $^{*}P < 0.05$, $^{**}P < 0.01$, $n \geq 4$.

and *Il1b* in bones, and that in BXSB-Yaa showed significant and negative correlations with S/B and *Il1a* and *Il1b* expression in bones. Tb.Wi showed significant and negative correlations with S/B, serum anti-dsDNA antibody levels, and the mRNA expression of *Rab9*, transcription elongation factor A (SII) N-terminal and central domain (*Tceanc*), *Tmsb4x*, *Tlr7*, *Tlr8*, *Prps2*, holocytochrome c synthase (*Hccs*), *Il1a*, and *Il1b* in bones, and that of BXSB-Yaa showed significant and negative correlations with oral-facial digital syndrome 1 (*Ofd1*), *Rab9*, *Tmsb4x*, *Il1a*, and *Il6* expression. The number of $TRAP^{+}$ osteoclasts showed significant and positive correlations with S/B, serum anti-dsDNA antibody levels, and mRNA expression of *Tlr8*, *Msl3*, *Arhgap6*, and *Mid1* in bones; and that in BXSB-Yaa showed significant and positive correlations with *Rab9* expression in bones. The numerical values of $osteocalcin^{+}$ osteoblast area showed significant and positive correlations with mRNA expression of *Amelx* in bones, and that in BXSB-Yaa showed significant and negative correlations with the *Tlr7* expression in bones.

Discussion

We clarified that the autoimmune disease-prone BXSB-Yaa had higher level of serum Ca at two to four months. Ca serum level is an indicator of bone metabolism, and

hypercalcemia is predominantly caused by osteoclast activation as found in human osteoporosis with advancing age or menopause.[30,31] In fact, BXSB-Yaa showed an increase in the number of $TRAP^+$ osteoclasts from three months. Further, at six months, the serum level and urinary excretion of Ca in BXSB-Yaa significantly decreased and increased, respectively, with the progression of autoimmune disease phenotypes including nephritis. Although the renal tubules play a crucial role in the Ca reabsorption from primitive urine, the Ca could not be reabsorbed through renal tubules in aged BXSB-Yaa because of renal injury. Notably, secondary renal hyperparathyroidism was observed to develop to compensate the increased urinary loss of Ca in the CKD patients.[16] However, there was no change in the serum PTH level as well as the morphologies of thyroid and parathyroid glands in BXSB-Yaa during the examined periods. Importantly, in aged BXSB-Yaa, the tibia length and the weight of tibia and fibula were observed to significantly decrease compared with BXSB. Therefore, altered Ca dynamics in BXSB-Yaa suggested that their osteoclast number was increased and activated via a PTH-independent mechanism as a direct consequence of autoimmune disease or *Yaa* mutations to bone metabolism.

Previous studies have reported the development of hemolytic anemia, one of the causes of osteoporosis, in mice carrying *Yaa* mutations.[32] Here, we also revealed that aged BXSB-Yaa showed higher and lower values in MCV and MCHC, respectively compared to BXSB. However, number of RBCs and Ht was comparable between both strains. A high value of MCV signifies the production of large and immature RBCs including reticulocytes in response to anemia.[33] MCHC indicated the hemoglobin concentration in RBC; generally, a reduced MCHC was followed by a decrease in the MCV as found in microcytic hypochromic anemia because of iron deficiency.[33] Alternatively, the altered patterns of MCV and MCHC in BXSB-Yaa were not typical cases of anemia. Importantly, we also found significantly increased numbers of WBCs and decreased PLs in aged BXSB-Yaa. Therefore, these data reflect that the altered hematopoiesis, such as abnormal lymphocyte production as shown in the previous study about human multiple myeloma,[34] might also affect the values of hemoanalysis and BM morphology in BXSB-Yaa.

BXSB-Yaa tended to show an increase in osteoclasts and decrease in osteoblasts in the tibia at three months. These altered populations to bone resorption patterns would be associated with the increased serum Ca level in BXSB-Yaa. Further, a sustained increase in osteoclast number from three to six months would be critical for the abnormal remodeling of bones, as characterized by significant reduction in bone length, weight, and trabeculas at six months. Importantly, the osteocyte number was not altered, however, the bone area was reduced in the tibia of BXSB-Yaa during periods of observation, indicating total decrease of osteocytes, important cells for mineral metabolism.[35] Along with PTH, inflammatory cytokines including IL-1, IL-6, and TNF-α can activate osteoclasts as found in the patients with RA and osteoporosis.[10–12] However, these cytokines were not significantly correlated with the indices for bone morphology and osteoclast numbers in the present study. Notably, in BXSB-Yaa, the numerical values of osteoblasts was rescued at six months of age. However, the functional maturation was not clear in the increased numerical values of osteoblasts in BXSB-Yaa. Thus, the hyperimmune status in BM would be induced by autoimmune abnormality, and it might indirectly affect the function and/or population of cells-associating bone remodeling in BXSB-Yaa. Importantly, similar pathological alterations characterized by the loss of bone tissue due to imbalance between osteoclasts and osteoblasts were observed in the osteoporosis patients.[6] The patients of autoimmune disease also develop osteoporosis, for example, RA in humans causes secondary osteoporosis due to inflammatory cytokines, medicine, or immobilization.[36] Therefore, BXSB-Yaa would be a suitable model to analyze the altered bone remodeling due to autoimmune abnormalities.

The causative factors of autoimmune disorder in BXSB-Yaa were encoded on the *Yaa* locus.[19] We examined the expression of all 15 protein-coding genes on this locus to discuss their pathological contributions of autoimmunity and bone morphology. At three months, *Rab9*, *Tmsb4x*, *Prps2*, *Tlr7*, and *Tlr8* were highly expressed in BXSB-Yaa bones. There was no relation between *Rab9* and autoimmunity. However, this gene was associated with osteoclast function to secrete lysosomal enzymes in rats.[37] *Tmsb4x* is a diagnostic indicator of osteoporosis or a regulator of the differentiation of hematopoietic cells in humans,[38,39] and these genes were also significantly correlated with the indices of bone area in BXSB-Yaa. *Prps2* also significantly correlated with the indices of bone area in BXSB-Yaa, and the variants of *Prps2* genes were associated with the development of SLE in humans,[40] however, there is no report on the bone. Furthermore, the associations of TLR7 or 8 and autoimmune abnormalities were well analyzed in BXSB-Yaa,[22,41] and the roles of candidate genes in developing SLE-like symptoms including nephritis were suggested. TLR7 was associated with RA by contributing to produce inflammatory cytokines, such as IL-1, IL-6, and TNF-α, from macrophages in mice.[42,43] TLR8 may have a role in human RA, however, the detailed function of murine TLR8 is unclear.[44] Therefore, these genes would be candidates to develop the autoimmune disease and/or following bone abnormalities.

The expression of *Msl3*, *Arhgap6*, *Amelx* and *Mid1* on *Yaa* locus significantly increased with the progression of the autoimmune disease. However, there is no evidence between *Msl3* or *Mid1* and autoimmunity or bones, but *Mid1* seemed to be associated with activating the innate immune pathway in allergic asthma.[45] Alternatively, human *Arhgap6*, activating the Ras homolog gene family, member A (RhoA),[46] and *Amelx* in mice seemed to act as the mediator of osteoblasts and osteoclasts-genesis, respectively.[47,48] Therefore, these genes would deteriorate autoimmune disease and/or bone abnormalities as exacerbating factors.

There were neither age- nor strain-related differences in the expression of *Ofd1*, *Tceanc*, and *Hccs*. However, the expression of these genes had significant and negative correlation with Tb.Wi. Additionally, *Ofd1* seemed to be associated with endochondral skeletal development,[49] although

there is no report of the evidence between *Tceanc* or *Hccs* and autoimmunity or bone study. Thus, these genes might also contribute to bone abnormality.

We have demonstrated that systemic autoimmune disease in BXSB-Yaa is closely associated with the morpho-functional abnormalities of bones including BM. The abnormalities are characterized by altered regulations of serum Ca, anemia tendency, and hematopoiesis with increased WBCs and decreased PLs, short length and low mass of long bones, imbalance in the populations of osteoclasts and osteoblasts, and increased expression of candidate genes for causing and/or exacerbating their phenotypes. Therefore, as shown in BXSB-Yaa, we concluded that the bone phenotypes in systemic autoimmune disease would elaborately be affected by the factors in the bone as well as the other immune and/or mineral metabolism organs.

AUTHORS' CONTRIBUTION

TaN, OI and YK designed and performed the experiments, and TeN, MAM, YO, SOK, and YHAE provided the samples and analyzed the data. All authors were involved in writing the paper and have approved the final manuscript.

DECLARATION OF CONFLICTING INTERESTS

The author(s) declared no potential conflicts of interest with respect to the research, authorship, and/or publication of this article.

FUNDING

The author(s) received no financial support for the research, authorship, and/or publication of this article.

ORCID iD

Teppei Nakamura http://orcid.org/0000-0003-3204-0245

REFERENCES

1. Calvi LM, Adams GB, Weibrecht KW, Weber JM, Olson DP, Knight MC, Martin RP, Schipani E, Divieti P, Bringhurst FR, Milner LA, Kronenberg HM, Scadden DT. Osteoblastic cells regulate the haematopoietic stem cell niche. *Nature* 2003;**425**:841–6
2. Teitelbaum SL, Ross FP. Genetic regulation of osteoclast development and function. *Nat Rev Genet* 2003;**4**:638–49
3. Anderson DM, Maraskovsky E, Billingsley WL, Dougall WC, Tometsko ME, Roux ER, Teepe MC, DuBose RF, Cosman D, Galibert L. A homologue of the TNF receptor and its ligand enhance T-cell growth and dendritic-cell function. *Nature* 1997;**390**:175–9
4. Wong BR, Rho J, Arron J, Robinson E, Orlinick J, Chao M, Kalachikov S, Cayani E, Bartlett FS, 3rd, Frankel WN, Lee SY, Choi Y. TRANCE is a novel ligand of the tumor necrosis factor receptor family that activates c-Jun N-terminal kinase in T cells. *J Biol Chem* 1997;**272**:25190–4
5. Johnell O, Kanis JA. An estimate of the worldwide prevalence and disability associated with osteoporotic fractures. *Osteoporos Int* 2006;**17**:1726–33
6. Rachner TD, Khosla S, Hofbauer LC. New horizons in osteoporosis. *Lancet Lond Lancet* 2011;**377**:1276–87
7. Villa A, Guerrini MM, Cassani B, Pangrazio A, Sobacchi C. Infantile malignant, autosomal recessive osteopetrosis: the rich and the poor. *Calcif Tissue Int* 2009;**84**:1–12
8. Firestein GS. Evolving concepts of rheumatoid arthritis. *Nature* 2003;**423**:356–61
9. Haugeberg G, Uhlig T, Falch JA, Halse JI, Kvien TK. Bone mineral density and frequency of osteoporosis in female patients with rheumatoid arthritis: results from 394 patients in the Oslo County rheumatoid arthritis register. *Arthritis Rheum* 2000;**43**:522–30
10. Arend WP, Dayer J-M. Inhibition of the production and effects of interleukins-1 and tumor necrosis factor α in rheumatoid arthritis. *Arthritis Rheum* 1995;**38**:151–60
11. Iwakura Y. Roles of IL-1 in the development of rheumatoid arthritis: consideration from mouse models. *Cytokine Growth Factor Rev* 2002;**13**:341–55
12. Liu X-H, Kirschenbaum A, Yao S, Levine AC. Cross-talk between the interleukin-6 and prostaglandin E_2 signaling systems results in enhancement of osteoclastogenesis through effects on the osteoprotegerin/receptor activator of nuclear factor-κB (RANK) ligand/RANK system. *Endocrinology* 2005;**146**:1991–8
13. Rossini M, Viapiana O, Adami S, Idolazzi L, Fracassi E, Gatti D. Focal bone involvement in inflammatory arthritis: the role of IL17. *Rheumatol Int* 2016;**36**:469–82
14. Peacock M. Calcium metabolism in health and disease. *Clin J Am Soc Nephrol* 2010;**5**:S23–30
15. Pondel M. Calcitonin and calcitonin receptors: bone and beyond. *Int J Exp Pathol* 2000;**81**:405–22
16. Saliba W, El-Haddad B. Secondary hyperparathyroidism: pathophysiology and treatment. *J Am Board Fam Med* 2009;**22**:574–81
17. Agmon-Levin N, Theodor E, Segal RM, Shoenfeld Y. Vitamin D in systemic and organ-specific autoimmune diseases. *Clinic Rev Allerg Immunol* 2013;**45**:256–66
18. Haywood MEK, Rogers NJ, Rose SJ, Boyle J, McDermott A, Rankin JM, Thiruudaian V, Lewis MR, Fossati-Jimack L, Izui S, Walport MJ, Morley BJ. Dissection of BXSB lupus phenotype using mice congenic for chromosome 1 demonstrates that separate intervals direct different aspects of disease. *J Immunol* 2004;**161**:2753–61
19. Pisitkun P, Deane JA, Difilippantonio MJ, Tarasenko T, Satterthwaite AB, Bolland S. Autoreactive B cell responses to RNA-related antigens due to TLR7 gene duplication. *Science* 2006;**312**:1669–72
20. Kawano S, Lin Q, Amano H, Kaneko T, Nishikawa K, Tsurui H, Tada N, Nishimura H, Takai T, Shirai T, Takasaki Y, Hirose S. Phenotype conversion from rheumatoid arthritis to systemic lupus erythematosus by introduction of *Yaa* mutation into FcγRIIB-deficient C57BL/6 mice. *Eur J Immunol* 2013;**43**:770–8
21. Kimura J, Ichii O, Otsuka S, Sasaki H, Hashimoto Y, Kon Y. Close relations between podocyte injuries and membranous proliferative glomerulonephritis in autoimmune murine models. *Am J Nephrol* 2013;**38**:27–38
22. Kimura J, Ichii O, Miyazono K, Nakamura T, Horino T, Otsuka-Kanazawa S, Kon Y. Overexpression of toll-like receptor 8 correlates with the progression of podocyte injury in murine autoimmune glomerulonephritis. *Sci Rep* 2014;**4**:7290
23. Kosenda K, Ichii O, Otsuka S, Hashimoto Y, Kon Y. BXSB/MpJ-*Yaa* mice develop autoimmune dacryoadenitis with the appearance of inflammatory cell marker messenger RNAs in the lacrimal fluid. *Clin Experiment Ophthalmol* 2013;**41**:788–97
24. Schneider CA, Rasband WS, Eliceiri KW. NIH Image to ImageJ: 25 years of image analysis. *Nat Methods* 2012;**9**:671–5
25. Parfitt AM, Drezner MK, Glorieux FH, Kanis JA, Malluche H, Meunier PJ, Ott SM, Recker RR. Bone histomorphometry: standardization of nomenclature, symbols, and units: report of the ASBMR Histomorphometry Nomenclature Committee. *J Bone Miner Res* 1987;**2**:595–610
26. Chen S, Li J, Peng H, Zhou J, Fang H. Administration of erythropoietin exerts protective effects against glucocorticoid-induced osteonecrosis of the femoral head in rats. *Int J Mol Med* 2014;**33**:840–8
27. Minkin C. Bone acid phosphatase: tartrate-resistant acid phosphatase as a marker of osteoclast function. *Calcif Tissue Int* 1982;**34**:285–90
28. Ducy P, Zhang R, Geoffroy V, Ridall AL, Karsenty G. Osf2/Cbfa1: a transcriptional activator of osteoblast differentiation. *Cell* 1997;**89**:747–54
29. Bendre MS, Montague DC, Peery T, Akel NS, Gaddy D, Suva LJ. Interleukin-8 stimulation of osteoclastogenesis and bone resorption is

a mechanism for the increased osteolysis of metastatic bone disease. *Bone* 2003;**33**:28–37
30. Jeremiah MP, Unwin BK, Greenawald MH. Diagnosis and management of osteoporosis. *Am Fam Physician* 2015;**92**:261–8
31. Riggs BL, Wahner HW, Seeman E, Offord KP, Dunn WL, Mazess RB, Johnson KA, Melton LJ. 3rd Changes in bone mineral density of the proximal femur and spine with aging. Differences between the post-menopausal and senile osteoporosis syndromes. *J Clin Invest* 1982;**70**:716–23
32. Moll T, Martinez-Soria E, Santiago-Raber M-L, Amano H, Pihlgren-Bosch M, Marinkovic D, Izui S. Differential activation of anti-erythrocyte and anti-DNA autoreactive B lymphocytes by the Yaa mutation. *J Immunol* 2005;**174**:702–9
33. Moreno Chulilla JA, Romero Colás MS, Gutiérrez Martín M. Classification of anemia for gastroenterologists. *World J Gastroenterol* 2009;**15**:4627–37
34. Sharma S, Nemeth E, Chen Y-H, Goodnough J, Huston A, Roodman GD, Ganz T, Lichtenstein A. Involvement of hepcidin in the anemia of multiple myeloma. *Clin Cancer Res* 2008;**14**:3262–7
35. Prideaux M, Findlay DM, Atkins GJ. Osteocytes: the master cells in bone remodelling. *Curr Opin Pharmacol* 2016;**28**:24–30
36. McLendon AN, Woodis CB. A review of osteoporosis management in younger premenopausal women. *Womens Health (Lond Engl)* 2014;**10**:59–77
37. Zhao H, Ettala O, Väänänen HK. Intracellular membrane trafficking pathways in bone-resorbing osteoclasts revealed by cloning and sub-cellular localization studies of small GTP-binding rab proteins. *Biochem Biophys Res Commun* 2002;**293**:1060–5
38. Borsy A, Podani J, Stéger V, Balla B, Horváth A, Kósa JP, Gyurján I, Jr, Molnár A, Szabolcsi Z, Szabó L, Jakó E, Zomborszky Z, Nagy J, Semsey S, Vellai T, Lakatos P, Orosz L. Identifying novel genes involved in both deer physiological and human pathological osteoporosis. *Mol Genet Genomics* 2009;**281**:301–13
39. Shimamura R, Kudo J, Kondo H, Dohmen K, Gondo H, Okamura S, Ishibashi H, Niho Y. Expression of the thymosin beta 4 gene during differentiation of hematopoietic cells. *Blood* 1990;**76**:977–84
40. Zhang Y, Zhang J, Yang J, Wang Y, Zhang L, Zuo X, Sun L, Pan HF, Hirankarn N, Wang T, Chen R, Ying D, Zeng S, Shen JJ, Lee TL, Lau CS, Chan TM, Leung AM, Mok CC, Wong SN, Lee KW, Ho MH, Lee PP, Chung BH, Chong CY, Wong RW, Mok MY, Wong WH, Tong KL, Tse NK, Li XP, Avihingsanon Y, Rianthavorn P, Deekajorndej T, Suphapeetiporn K, Shotelersuk V, Ying SK, Fung SK, Lai WM, Wong CM, Ng IO, Garcia-Barcelo MM, Cherny SS, Tam PK, Sham PC, Yang S, Ye DQ, Cui Y, Zhang XJ, Lau YL, Yang W. Meta-analysis of GWAS on two Chinese populations followed by replication identifies novel genetic variants on the X chromosome associated with systemic lupus erythematosus. *Hum Mol Genet* 2015;**24**:274–84
41. Santiago-Raber M-L, Kikuchi S, Borel P, Uematsu S, Akira S, Kotzin BL, Izui S. Evidence for genes in addition to Tlr7 in the Yaa translocation linked with acceleration of systemic lupus erythematosus. *J Immunol* 2008;**181**:1556–62
42. Alzabin S, Kong P, Medghalchi M, Palfreeman A, Williams R, Sacre S. Investigation of the role of endosomal toll-like receptors in murine collagen-induced arthritis reveals a potential role for TLR7 in disease maintenance. *Arthritis Res Ther* 2012;**14**:R142
43. Huang Q-Q, Pope RM. The role of toll-like receptors in rheumatoid arthritis. *Curr Rheumatol Rep* 2009;**11**:357–64
44. Sacre SM, Lo A, Gregory B, Simmonds RE, Williams L, Feldmann M, Brennan FM, Foxwell BM. Inhibitors of TLR8 reduce TNF production from human rheumatoid synovial membrane cultures. *J Immunol* 2008;**181**:8002–9
45. Collison A, Hatchwell L, Verrills N, Wark PA, de Siqueira AP, Tooze M, Carpenter H, Don AS, Morris JC, Zimmermann N, Bartlett NW, Rothenberg ME, Johnston SL, Foster PS, Mattes J. The E3 ubiquitin ligase midline 1 promotes allergen and rhinovirus-induced asthma by inhibiting protein phosphatase 2A activity. *Nat Med* 2013;**19**:232–7
46. Prakash SK, Paylor R, Jenna S, Lamarche VN, Armstrong DL, Xu B, Mancini MA, Zoghbi HY. Functional analysis of ARHGAP6, a novel GTPase-activating protein for RhoA. *Hum Mol Genet* 2000;**9**:477–88
47. McBeath R, Pirone DM, Nelson CM, Bhadriraju K, Chen CS. Cell Shape, cytoskeletal tension, and RhoA regulate stem cell lineage commitment. *Dev Cell* 2004;**6**:483–95
48. Jacques J, Hotton D, De la Dure-Molla M, Petit S, Asselin A, Kulkarni AB, Gibson CW, Brookes SJ, Berdal A, Isaac J. Tracking endogenous amelogenin and ameloblastin in vivo. *PLoS One* 2014;**9**:e99626
49. Bimonte S, De Angelis A, Quagliata L, Giusti F, Tammaro R, Dallai R, Ascenzi MG, Diez-Roux G, Franco B. Ofd1 is required in limb bud patterning and endochondral bone development. *Dev Biol* 2011;**349**:179–91

(Received November 30, 2018, Accepted January 31, 2019)